MOLECULAR AND CELLULAR BIOLOGY, Apr. 2007, p. 2499–2511 Vol. 27, No. 7
0270-7306/07/$08.00+0 doi:10.1128/MCB.01088-06

Phenotypes Developed in Secretin Receptor-Null Mice Indicated a Role for Secretin in Regulating Renal Water Reabsorption▽

Jessica Y. S. Chu,[1]† Samuel C. K. Chung,[1]† Amy K. M. Lam,[2] Sidney Tam,[3] Sookja K. Chung,[2] and Billy K. C. Chow[1]*

Department of Zoology,[1] Department of Anatomy,[2] and Division of Clinical Biochemistry,[3] The University of Hong Kong, Pokfulam, Hong Kong SAR, China

Received 16 June 2006/Returned for modification 21 July 2006/Accepted 14 December 2006

Aquaporin 2 (AQP2) is responsible for regulating the concentration of urine in the collecting tubules of the kidney under the control of vasopressin (Vp). Studies using Vp-deficient Brattleboro rats, however, indicated the existence of substantial Vp-independent mechanisms for membrane insertion, as well as transcriptional regulation, of this water channel. The Vp-independent mechanism(s) is clinically relevant to patients with X-linked nephrogenic diabetes insipidus (NDI) by therapeutically bypassing the dysfunctional Vp receptor. On the basis of studies with secretin receptor-null (*SCTR*$^{-/-}$) mice, we report here for the first time that mutation of the *SCTR* gene could lead to mild polydipsia and polyuria. Additionally, *SCTR*$^{-/-}$ mice were shown to have reduced renal expression of AQP2 and AQP4, as well as altered glomerular and tubular morphology, suggesting possible disturbances in the filtration and/or water reabsorption process in these animals. By using *SCTR*$^{-/-}$ mice as controls and comparing them with wild-type animals, we performed both in vivo and in vitro studies that demonstrated a role for secretin in stimulating (i) AQP2 translocation from intracellular vesicles to the plasma membrane in renal medullary tubules and (ii) expression of this water channel under hyperosmotic conditions. The present study therefore provides information for at least one of the Vp-independent mechanisms that modulate the process of renal water reabsorption. Future investigations in this direction should be important in developing therapeutic means for treating NDI patients.

Secretin was originally isolated from upper intestinal mucosal extract, injection of which into the jugular vein of an anesthetized dog resulted in elevation of pancreatic and hepatic bile flow (4). The primary function of secretin in releasing bicarbonate, electrolytes, and water from pancreatic ductal epithelial cells is firmly established. Additionally, it can also stimulate electrolyte and water secretion in the epididymis, as well as bicarbonate-rich ductal bile secretion from cholangiocytes (1, 9). In cholangiocytes, a secretin-induced choleretic effect is associated with microtubule-dependent exocytotic insertion of cytoplasmic vesicles containing the water channel aquaporin 1 (AQP1) onto the apical plasma membrane (PM), leading to osmotic water movement (28). Interestingly, this type of regulated translocation of water channels has also been demonstrated in other cell types (5). For example, vasoactive intestinal polypeptide-induced translocation of AQP5 in Brunner's gland of the duodenum is associated with bicarbonate and mucin secretion, which is essential for mucosal protection (38), while Vp- and oxytocin-triggered translocation of AQP2 to and from the PM in renal collecting tubules (19, 36) is critical for renal water reabsorption. As there is considerable evidence indicating the involvement of Vp-independent mechanisms in the regulation of renal water reabsorption (19, 21, 25, 44) and some of these mechanisms are associated with cyclic-AMP (cAMP)–protein kinase A-mediated phosphorylation of water channels, we hypothesized that secretin could modulate renal water permeability by inducing Vp-independent translocation of functional AQP2 in a similar way as in cholangiocytes. For these reasons, we focused on the in vivo functions of secretin in the urinary systems of our recently generated secretin receptor knockout (*SCTR*$^{-/-}$) mice. We report here for the first time that, by comparison of knockout and wild-type animals, we found that secretin might play a modulatory role in water reabsorption in the renal tubules.

MATERIALS AND METHODS

Cloning of the mouse secretin receptor. Adult 129Sv mice were sacrificed by cervical dislocation. The pancreases were quickly excised and homogenized in TRIZOL reagent (Invitrogen, San Diego, CA). Total RNA was extracted and used (5 μg) to synthesize first-strand cDNAs with Superscript System III (Invitrogen). Initially, primers hSRQ2 and hSRQ3 (Table 1) were designed to amplify a partial receptor clone, which spans transmembrane domain 2 to the third intracellular loop. To clone the full-length receptor, 5′ and 3′ rapid amplification of cDNA ends (RACE) was performed with first-strand cDNA synthesized by AUAP-tagged-oligo(dT)s and primer 5′RACE-R1, respectively. For 5′ RACE, first-strand cDNAs were purified by a GFX DNA and gel purification kit (Amersham) and then processed by TdT tailing. The 5′ RACE products were produced by amplification with primers 5′RACE-R2 or 5′RACE-R3 or 5′RACE-R4 and ANP. 3′ RACE was performed with primers 3′RACE-F1 or 3′RACE-F2 and AUAP. After sequencing of the 5′ and 3′ RACE products, the full-length cDNA encoding the entire coding region of murine *SCTR* (m*SCTR*) was amplified by mSR-ATG and mSR-TGA. This 1.75-kb PCR product was sequenced and subcloned into the HindIII and XbaI sites of the expression vector pRcCMV (Invitrogen) for functional studies. An *SCTR* mutant that lacks the sequence encoded by exon 10 was generated by a three-step PCR mutagenesis method (22) with primers mSR-Exons9&11, mSR-TGA, mSR-ATG, and mSR-Exon9 (Table 1) and subcloned into the HindIII and XbaI sites of pRcCMV.

* Corresponding author. Mailing address: Department of Zoology, The University of Hong Kong, Pokfulam, Hong Kong SAR, China. Phone: 852-22990850. Fax: 852-25599114. E-mail: bkcc@hkusua.hku.hk.

† J. Y. S. Chu and S. C. K. Chung contributed equally to the overall design and execution of the experiments described here.

▽ Published ahead of print on 5 February 2007.

TABLE 1. Oligonucleotides used in this study

Primer name	Sequence (5′→3′)[a]
hSRQ2	GCCCTGTCCAACTTCATCAAGGACGCC
hSRQ3	GGCCAGGCGCTTATAATG
3′RACE-F1	CCAGTACTGCATCATGGCCAAC
3′RACE-F2	GGTGCAGCTGGAAGTTCAGA
5′RACE-R1	AGTAGGTGACGTCATCTGCGG
5′RACE-R2	ATGACCTTGAGCTTCAGCAG
5′RACE-R3	AGGCCTGGGGAAGGTTTCTG
5′RACE-R4	CTGATGCTGTCTTCGGGCCCAG
AAP	GGCCACGCGTCGACTAGTACGGGGGGGGGGGGGGGG
AUAP	GGCCACGCGTCGACTAGTAC
mSR-ATG	ACCTAAGCTTAACAGTGGGCGGAGCATGCTC
mSR-TGA	CCCTTCTAGAGCTGCAGCCTCAGATGACAT
mSR-Exons9&11	AGGGCCTGTGATTCTGTCCATCGTGGCGCCTGGCCAAGTCCACCCTCCTG
mSR-Exon9	GATGGACAGAATCACAGGCCCTCG
mSRcfc-R1	TACTCTAGAGATGACATTGGCCCCGGGGAT
jpxb	CCATGGCTCAGGCAAGCC
jpxh	GCCTGAGGTTTCATACTCAGGCCC
jpxE	GGATAATGCTAGCCATGTTTGGGG
tkF1	GCCAAGACGTCCAAAGCCCAGGC
neoF1	GCTACTTCCATTTGTCACGTCCTG
neoR1	GATCAGCAGCCTCTGTTCCAC
mGAPDH-F	GGAGAAACCTGCCAAGTA
mGAPDH-R	AAGAGTGGGAGTTGCTGTTG
AQP2-F	CTGGTGCTGTGCATCTTTGC
AQP2-R	ATGGAGCAGCCGGTGAAAT
AQP4-F	ACCATAAACTGGGGTGGCTCAG
AQP4-R	TTTCGTGTGCACACCATGGCTA
mSCT-F	GACCATGGAGCCTCCGCTG
mSCT-R	GGGACAGCCTGGGCAGAAGCC
V2R-F	ATGATCCTGGTGTCTACCACGTCT
V2R-R	TGAAGACGTGCATGGGTGCCCA
IL-10-F	CAGCCTTGCAGAAAAGAGAG
IL-10-R	GGAAGTGGGTGCAGTTATTG
TGF-β1-F	CTCCACCTGCAAGACCAT
TGF-β1-R	CTTAGTTTGGACAGGATCTG
TNF-α-F	CGCTCTTCTGTCTACTGAACTT
TNF-α-R	GATGAGAGGGAGGCCATT
E-selectin-F	AGCTACCCATGGAACACGAC
E-selectin-R	CGCAAGTTCTCCAGCTGTT
OPN-F	TCCAATCGTCCCTACAGTCG
OPN-R	CCTTTCCGTTGTTGTCCTG

[a] The underlined sequences indicate the introduction of restriction enzyme cut sites for cloning.

cAMP assay. The wild-type and mutant m*SCTR* genes were functionally tested by cAMP assays. These clones were transfected separately into Chinese hamster ovary (CHO) cells (American Type Culture Collection, Manassas, VA) cultured in minimum essential medium supplemented with 10% fetal bovine serum, 100 U/ml penicillin, and 100 μg/ml streptomycin (Invitrogen) at 37°C in a 5% CO_2 incubator. For transient transfection, 2×10^5 cells/well were seeded into six-well plates (Costar, San Diego, CA) 48 h before transfection. Thereafter, 2 μg of receptor DNA construct and 1.5 μg of plasmid pCMV-SPORT-βgal were co-transfected into the cells with Lipofectamine reagent (Invitrogen) according to the manufacturer's protocol. Two days later, transfected cells were incubated with culture medium containing 0.2 mM 3-isobutyl-L-methylxanthine (Sigma, St. Louis, MO) for 30 min, stimulated with various concentrations of secretin (10^{-12} to 10^{-6} M) or 10^{-6} M forskolin for 45 min at 37°C, and lysed with 1 ml of ice-cold ethanol. Cell lysate was used for both cAMP (cAMP [^{125}I] radioimmunoassay kit; NEN Life Science Products Inc., Boston, MA) and galactosidase activity (31) assays.

Cellular localization of wild-type and mutant mSCTR in CHO cells. To locate wild-type and mutant mSCTR in transfected cells, cDNAs produced by PCR with primers mSR-ATG and mSRcfc-R1 were inserted into the HindIII and XbaI sites of pcDNA3.1/myc-HisA (Invitrogen), a c-Myc-tagged expression vector, for immunofluorescence studies. CHO cells were cultured on 12-mm glass coverslips and transiently transfected with the c-Myc-tagged receptor constructs. Two days after transfection, cells were fixed with 0.5% paraformaldehyde and permeabilized with phosphate-buffered saline-saponin. After addition of mouse anti-c-Myc monoclonal antibody (9E10; 1:250 dilution; Fisher Scientific Inc.) for 20 h of incubation at 4°C, the cells were washed and incubated with Cy-2 labeled rabbit anti-mouse immunoglobulin G (IgG; 1:200 dilution; Amersham), and the receptors were visualized by confocal microscopy (MRC 600; Bio-Rad Laboratories, Richmond, CA).

Construction of *SCTR* targeting vector and selection in embryonic stem (ES) cells. A murine 129Sv genomic DNA library (lambda FIX II library of ES cells at day 3; Stratagene, La Jolla, CA) was screened for the m*SCTR* gene with the full-length cDNA as the probe (Megaprime DNA labeling kit [Amersham Pharmacia, Buckinghamshire, England]; [α-^{32}P]dCTP, 3,000 Ci/mmol [Amersham Pharmacia]). Phage DNA was extracted from positive tertiary clones by the QIAGEN Lambda Midi Kit (QIAGEN Inc., Santa Clarita, CA), and a 22-kb genomic clone containing part of the m*SCTR* gene was isolated within which the 7.57-kb XhoI DNA fragment, which spans the region from exon 8 to exon 11, was used to construct the *SCTR* targeting vector.

A 5.05-kb XbaI/XbaI fragment which contains a part of intron 7 to a part of intron 9 of the m*SCTR* gene was inserted upstream of the thymidine kinase (*tk*) gene in gene replacement targeting vector pPNT. A PCR-generated 1.8-kb XhoI/NotI DNA fragment including exon 11 and a portion of introns 10 and 11 was inserted upstream of the neomycin resistance (*neo*) gene. This *SCTR* targeting vector, designated pPNT-SCTRko, with the PGK-1 promoter and *neo* replacing exon 10, was linearized with NotI and electroporated into 129Sv (AB2.2) mouse ES cells. By positive-negative selection, ES cell clones resistant to G418 and fialuridine (Sigma) were expanded in 96-well plates and then screened by two independent PCRs, one detecting the presence of the *neo* gene, with primers jpxb and neoR1, and the other detecting the absence of the *tk* gene, with primers jpxE and tkF1. Genomic DNA from the positive clones was digested with StuI and confirmed by Southern blot analysis. The 9.139-kb band in the blot denoted the presence of wild-type *SCTR*, whereas the 5.142-kb band indicated the presence of a mutated *SCTR* gene (Fig. 1B).

Animal handling. All experiments were carried out with adult mice (18 to 25 g), which were kept in a daily 12-h light–12-h dark cycle with free access to standard chow and water unless stated otherwise. Two independent 129Sv (AB2.2) ES cell clones with homologous recombination were microinjected into C57BL/6 blastocysts, which were transferred to pseudopregnant females to generate chimeric mice. Engendered mouse lines were then bred separately with female C57BL/6 mice to give F_1N_1 offspring. F_1N_1 heterozygous siblings were backcrossed through four generations with female C57BL/6 mice to produce heterozygous mice, which were inbred to obtain +/+, +/−, and −/− mice. The genotype of each mouse was confirmed by PCR amplification of genomic DNA extracted from the tail. The presence of a 564-bp band amplified from primers jpxb and jpxh denoted the presence of the wild-type *SCTR* gene, whereas a 396-bp band amplified from primers neoF1 and jpxh indicated the presence of a mutated *SCTR* gene (Fig. 1C). All of the mice examined in this study were of the N5 generation with 99.61% purity in their genetic background.

For measuring water consumption and urine output, mice were kept individually in metabolic cages. For water deprivation experiments, water bottles were removed for 2 days. Urine samples were collected by spontaneous voiding before and after the water-deprived period, and kidneys were isolated for the preparation of PM- and intracellular-vesicle (IV)-enriched fractions.

Assays for electrolytes, vasopressin (Vp), and secretin. Urine samples were collected from metabolic cages in a 24-h period, and serum samples were collected by cardiac puncture under basal conditions (unrestricted access to food and water). Urine Na, K, Ca, Cl, urea, and creatinine levels were measured with a Synchron CX5 analyzer (Beckman Instruments, Inc., Fullerton, CA). Serum Na, K, Ca, Cl, urea, and creatinine levels were measured with a Hitachi-747 autoanalyzer (Roche Diagnostics). Urine osmolality was measured by the vapor pressure method, with a Vapro vapor pressure osmometer (Wescor Inc., Logan, Utah). Serum osmolality was measured by the freezing depression method, with an Advanced Micro-Osmometer 3300 (Advanced Instruments, Inc.). Urine and serum Vp levels were measured with a Vp enzyme immunoassay kit (Assay Designs Inc., Ann Arbor, MI). Serum secretin levels were measured with a secretin enzyme immunoassay kit (Phoenix Pharmaceuticals, Inc., Belmont, CA).

Quantitative analyses of renal gene expression. The expression levels of various genes were measured by real-time PCR with a SYBR green PCR kit (Applied Biosystems). The gene for glyceraldehyde-3-phosphate dehydrogenase was used as an internal standard for normalization, and transcript levels of each gene were quantified with the iCycler iQ Detection System (Bio-Rad, Hercules, CA) according to the manufacturer's instructions. Fluorescence signals were measured at the extension step throughout the amplification process. The specificity of the fluorescence signal was confirmed by melting curve analysis and agarose gel electrophoresis. The threshold cycle (Ct) was determined for each sample and was defined as the fractional cycle number at which the fluorescence signals reached 10 times the standard deviation of the baseline. The expression level of the target gene was determined by the $2^{-\Delta\Delta Ct}$ method (24).

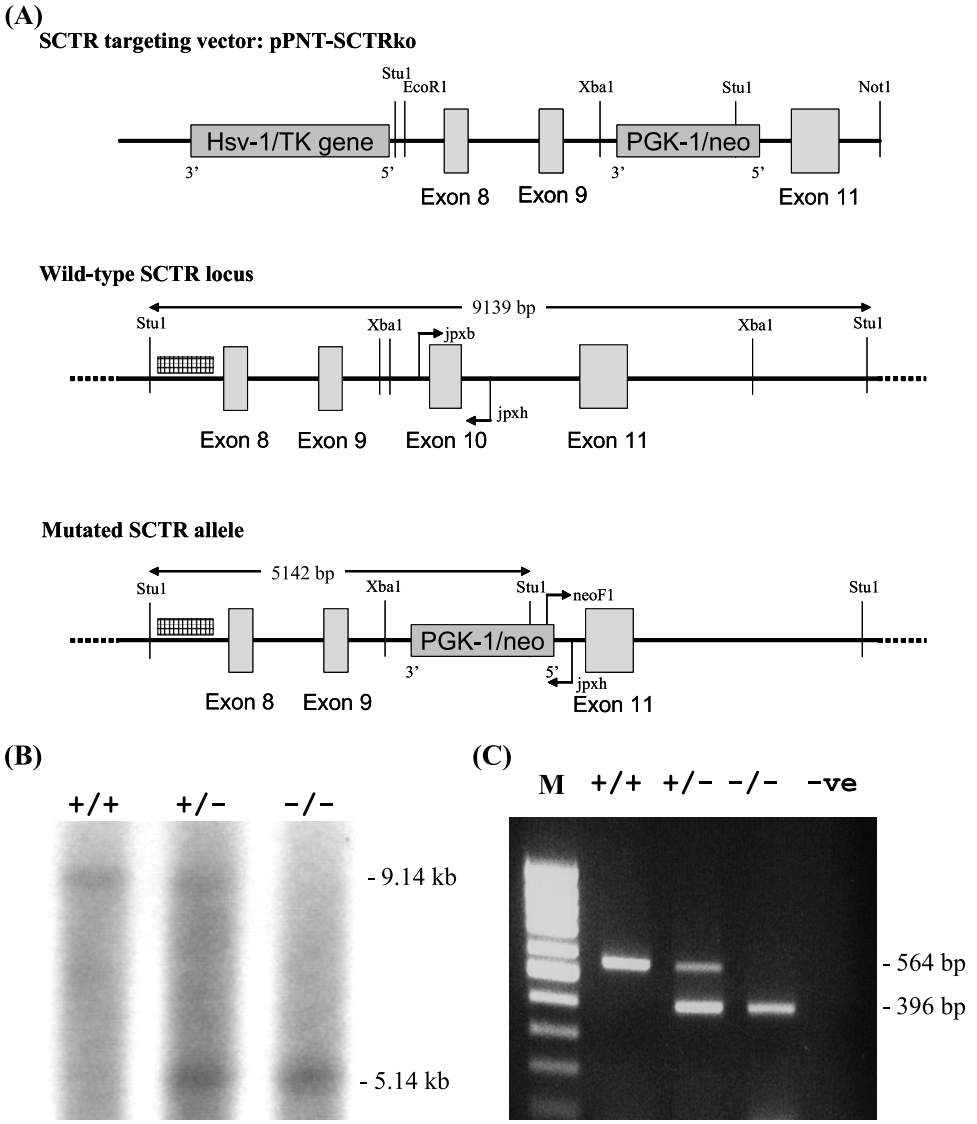

FIG. 1. (A) Targeted disruption of the m*SCTR* gene by homologous recombination. Schematic drawings of the pPNT-SCTRko vector, wild-type *SCTR* locus, and mutated *SCTR* allele. Exons 8, 9, 10, and 11 are indicated by closed boxes. The 5′ external probe for Southern blot analysis is represented by an oblong gray box, whereas the PCR primers for screening the wild-type and mutated *SCTR* alleles are represented by arrows. PGK-1/neo, phosphoglycerate kinase 1 promoter/neomycin resistance gene; Hsv-1/TK, herpes simplex virus type 1 promoter/thymidine kinase gene. (B) Southern blot analysis of genomic DNA extracted from mouse tail. The wild-type, heterozygous, and knockout genotypes were identified with a 5′ external probe. The 9.139-kb band and 5.142-kb band denote the presence of the wild-type and mutated *SCTR* genes, respectively. (C) Mutliplex PCR screening of genomic DNA extracted from mouse tail. The 564-bp band, amplified by primers jpxb and jpxh, denotes the presence of the wild-type *SCTR* allele, whereas the 396-bp band, amplified by primers neoF1 and jpxh, denotes the presence of a mutated *SCTR* allele.

Morphological analysis and immunofluorescence staining. For morphological analysis, kidneys from $SCTR^{+/+}$ and $SCTR^{-/-}$ mice were fixed in 4% paraformaldehyde, embedded in paraffin, sectioned (5 to 7 μm), and stained with hematoxylin and eosin and periodic acid-Schiff. For immunohistochemical staining, after deparaffinization, rehydration, and permeabilization in KPBS-BT (200 mg/liter KCl-containing phosphate-buffered saline supplemented with 0.25% bovine serum albumin and 0.1% Triton X-100), sections were blocked in a 12% donkey serum solution and incubated overnight with the primary antibody. For single-antigen staining, a primary antibody against mouse F4/80 (1:50 dilution; rat anti-mouse F4/80 antigen-fluorescein isothiocyanate; Serotec, Oxford, United Kingdom) was applied and sections were washed with KPBS-BT and mounted with 90% glycerol on the next day. For double-immunofluorescence staining, sections were incubated overnight with goat antiserum against AQP2 or the Vp type 2 receptor (V2R) (1:400 dilution; Santa Cruz Biotechnology, Inc.), washed in KPBS-BT, and incubated with Alexa Fluor 488 donkey anti-goat IgG (1:500 dilution; Molecular Probes Inc., Invitrogen). Chicken serum (12%) was then applied, and sections were incubated at 4°C overnight with rabbit anti-mouse secretin receptor antibody (1:200; recently raised in our laboratory with a synthetic peptide [R-A-E-C-L-R-E-L-S-E-E-K-K] that is present in the mouse secretin receptor) (9), followed by the addition of Alexa Fluor 594 chicken anti-rabbit IgG (1:500 dilution; Molecular Probes). Images were observed and captured with the Leica Quantimet 570 computerized image analysis system. To test the specificity of secretin receptor immunostaining, control experiments were performed with renal sections from $SCTR^{-/-}$ mice or by liquid phase preabsorption of the antiserum with the synthetic immunizing peptide (0.1 M) for 3 h at room temperature.

Tubule isolation and preparation of membrane fractions. $SCTR^{-/-}$ and $SCTR^{+/+}$ mice (8 to 9 weeks old) were killed by cervical dislocation. Kidneys

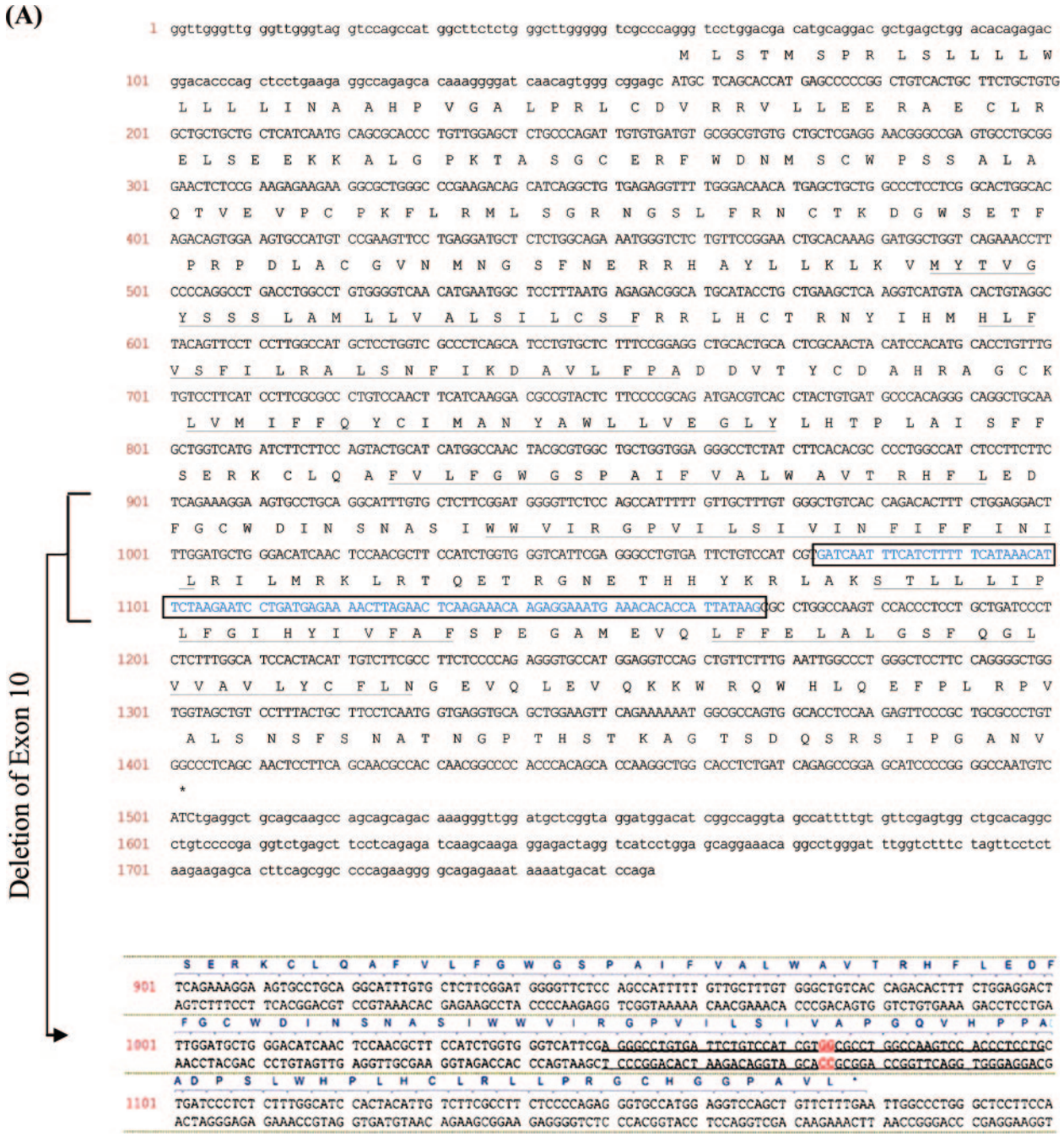

FIG. 2. The top part of panel A shows nucleotide and predicted amino acid sequences of the mouse *SCTR* cDNA. The number to the left of each row is the nucleotide position. The coding region is in capital letters, and the stop codon is marked by an asterisk. Transmembrane domains are underlined, and sequences encoded by exon 10 are shaded and boxed. The bottom part of panel A shows that deletion of exon 10 by primer mSR-Exons9&11 (underlined sequences) causes a frameshift in the open reading frame, introducing a premature stop codon. (B and C) Functional expression of wild-type and mutant *SCTR* genes in CHO cells. (B) Secretin dose dependently activates wild-type *SCTR* (WT-mSR) but not mutated *SCTR* (Mut-mSR). Changes in cAMP levels in response to increasing secretin doses (10^{-12} to 10^{-6} M) were measured in transiently transfected CHO cells. Data are represented as the mean ± the SEM. The inset shows the effect of 10^{-6} M forskolin on cAMP production in wild-type and mutant *SCTR*-transfected CHO cells. A 10^{-6} M forskolin concentration could stimulate 5.85-fold and 5.27-fold increases in cAMP production in WT-mSR-expressing and Mut-mSR-expressing CHO cells, respectively. (C) Confocal laser scanning microscopic detection of c-Myc-tagged SCTR. Wild-type (WT) SCTR could be translocated and expressed on the transfected-cell surface; whereas mutant *SCTR*, with the deletion of exon 10 that created a frameshift mutation and a termination codon beyond exon 9, could not be expressed in the respective cells. A control experiment was performed with vector-transfected CHO cells. Scale bars, 20 μm.

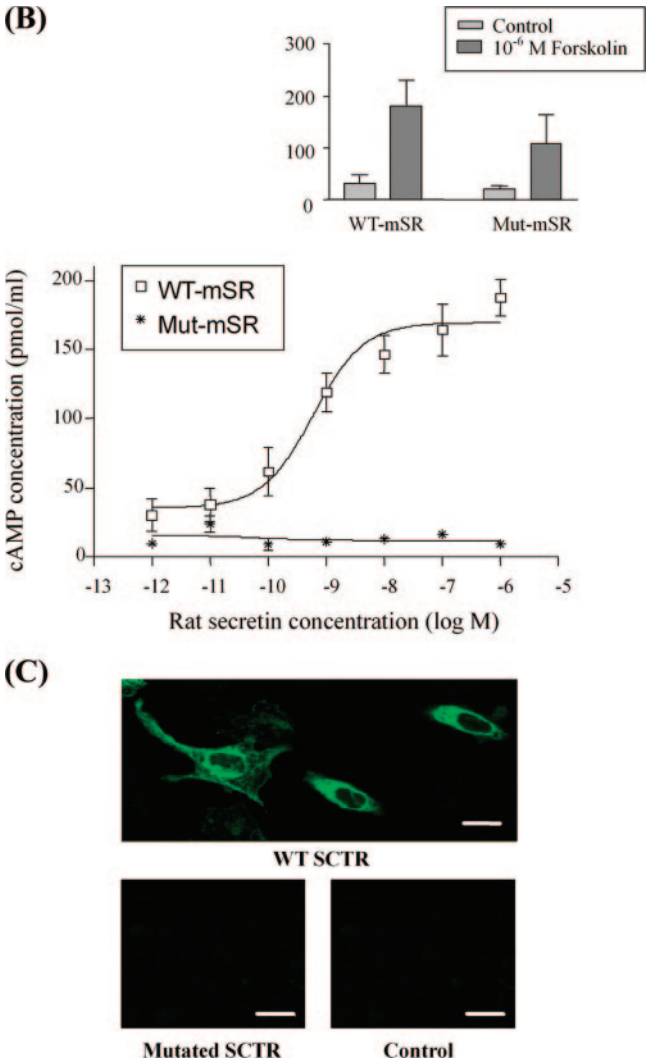

FIG. 2—*Continued*.

were rapidly removed; the inner medulla was dissected and finely minced with a razor blade. Ten milliliters of an enzymatic solution (Dulbecco modified Eagle medium-F12 containing 2 mg/ml collagenase, 1 mg/ml hyaluronidase, 0.1 mg/ml pronase, 4.8 mg/ml urea, 7.4 mg/ml NaCl, and 140 mM K-gluconate) was added, and the mixture was incubated at 37°C for 90 min in a shaking water bath top gassed with 95% CO_2–5% O_2. Thereafter, tubules were pelleted at 800 × *g* and resuspended in Leibovitz L-15 culture medium containing 80 mM urea and 1% bovine serum albumin. These centrifugation and resuspension steps were repeated three times to remove residual proteases. The kidney tubule preparation was then aliquoted into six-well plates with Leibovitz culture medium topped up to 3 ml with or without 30 min of secretin stimulation at 37°C. After drug treatment, the tubule preparation was pelleted at 800 × *g* and resuspended in 1 ml of ice-cold isolation solution (250 mM sucrose, 25 mM imidazole, and 10 mM tetraethylammonium with 1 μg/ml leupeptin and 1 mg/ml phenylmethylsulfonyl fluoride). Samples were homogenized and centrifuged at 4,000 × *g* for 15 min at 4°C to remove large cellular organelles, and the supernatant was collected and recentrifuged at 17,000 × *g* at 4°C for 30 min to obtain the PM (pellet) and IV (supernatant) fractions.

To assess the functional integrity of secretin receptors after enzymatic digestion in the isolation procedure, the kidney tubule preparation was stimulated with graded concentrations of secretin (10^{-10} to 10^{-6} M), followed by cAMP assay.

Western blot and densitometry analyses. Kidneys from *SCTR*$^{-/-}$ and *SCTR*$^{+/+}$ mice were homogenized and centrifuged at 4,000 × *g* for 15 min at 4°C. Protein concentration was determined, and the expression levels of AQP1, -2, -3, and -4 were measured by Western blotting, followed by densitometric analysis. Protein samples were separated in parallel in two 12% sodium dodecyl sulfate-polyacrylamide minigels. One gel was stained with Coomassie blue, and the other gel was used for immunoblotting.

For analyzing AQP2 expression after secretin treatment, PM fractions were loaded at 9 μg/well and IV fractions were loaded at 50 μg/well. This arrangement gave similar intensities of the AQP2 bands; thus, a more accurate estimation of the PM-to-IV ratio could be obtained. To measure various AQP levels in crude protein extracts prepared from wild-type and knockout animals, samples (9 μg/well) were separated in minigels and transferred onto Hybond-C extra nitrocellulose membranes (Amersham Biosciences) by electroelution for 2 h at 100 V with a Bio-Rad Mini Protean II transblot apparatus. The blots were blocked for 1 h with 5% skim milk in PBST (80 mM Na_2HPO_4, 20 mM NaH_2PO_4, 100 mM NaCl, 0.1% Tween 20, pH 7.5) and then incubated overnight at 4°C with the appropriate antibody (1:200 AQP1, 1:430 AQP2, 1:500 AQP3, or 1:200 AQP4; Santa Cruz Biotechnology, Santa Cruz, CA). After three washes in PBST, the blots were incubated for 1 h with horseradish peroxidase-conjugated secondary antibody against rabbit or goat IgG (1:8,000 or 1:5,800 dilution, respectively). Positive signals were produced by the enhanced chemiluminescence system (Amersham Biosciences), and enhanced chemiluminescence films were scanned and analyzed with the Easygel software to give the PM/IV ratio.

Statistical analysis. For quantitative real-time PCR analysis, data are shown as the mean ± the standard error of the mean (SEM) from at least three independent experiments, each in triplicate. All data were analyzed by one-way analysis of variance, followed by a Dunnett test with the computer software PRISM (version 3.0; GraphPad Software Inc., San Diego, CA). For metabolic experiments and expression studies, statistical significance was determined with the unpaired Student *t* test.

RESULTS

Targeted disruption of *SCTR*. *SCTR*$^{-/-}$ mice were generated by replacing exon 10 of the gene with a PGK-1 promoter–neomycin resistance gene cassette (Fig. 1). As indicated in previous studies that demonstrated the importance of the third endoloop in cell surface presentation and receptor maturation and stability (6), targeted disruption of exon 10, which encodes the third endoloop, should greatly hamper receptor function. Moreover, deletion of exon 10 also led to a frameshift of the m*SCTR* gene (Fig. 2A), hence introducing a premature stop codon. In conclusion, targeted deletion of exon 10 should produce a nonfunctional receptor.

To confirm the effect of exon 10 deletion on *SCTR* function, full-length mouse *SCTR* cDNA was isolated and subsequently used for constructing a mutant *SCTR* gene that lacks exon 10. The m*SCTR* cDNA contains an open reading frame of 1,347 bp and encodes a protein of 449 amino acids (Fig. 2A). Hydropathic analysis of the predicted sequences revealed a putative signal peptide of 28 amino acids, a large extracellular N terminus of 143 amino acids, and seven hydrophobic domains separated by stretches of hydrophilic amino acids, a feature characteristic of G protein-coupled receptors. By sequence comparison, this receptor is closely related to human and rat *SCTR* genes, sharing 81.4% and 91.1% sequence identity, respectively. The identity of this receptor is further confirmed by functional studies in which secretin, but not other, related peptides, could dose dependently stimulate this receptor in making cAMP (Fig. 2B) with a 50% inhibitory concentration of 10^{-10} M. On the other hand, the m*SCTR* mutant gene was totally nonfunctional when transiently transfected into CHO cells (Fig. 2B and C). Confocal images of the transfected cells clearly showed that the mutant was unable to present itself to the cell surface, although even if it were to translocate properly, without the KLR G-protein coupling motif in the third intracellular loop and with the introduction of the premature

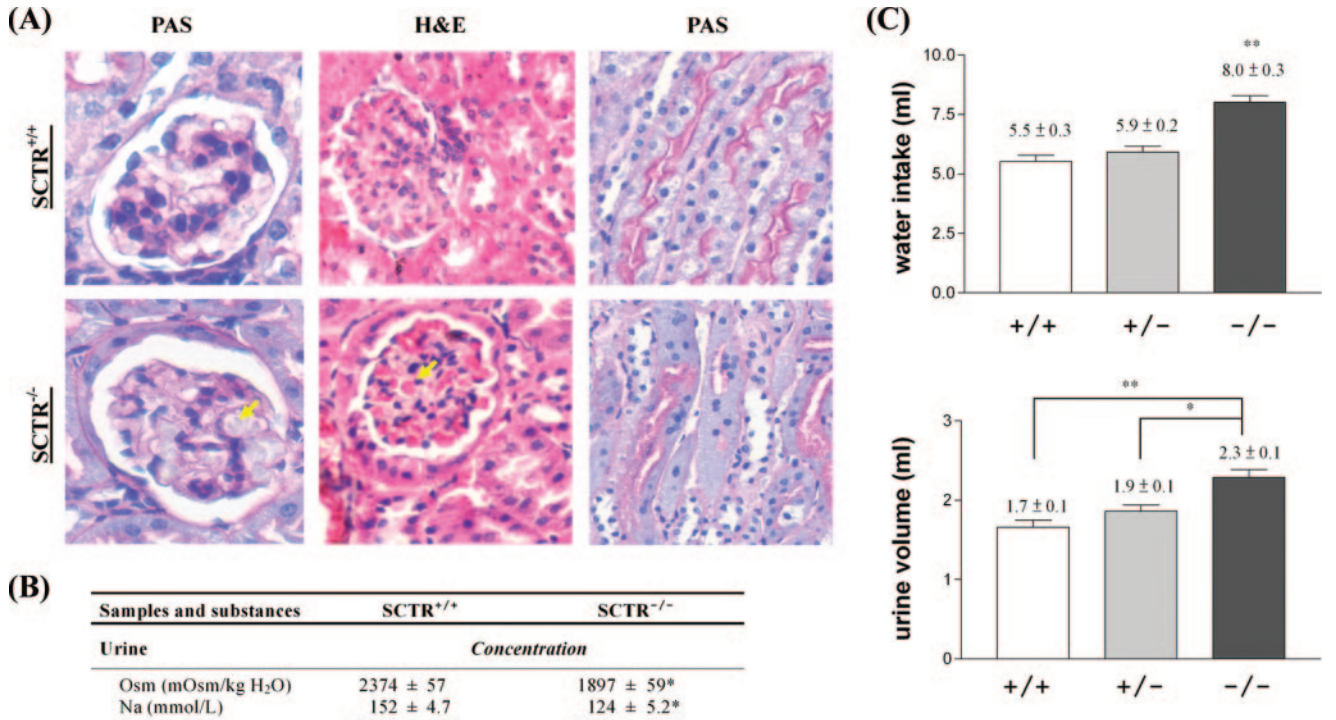

(B)

Samples and substances	$SCTR^{+/+}$	$SCTR^{-/-}$
Urine	*Concentration*	
Osm (mOsm/kg H_2O)	2374 ± 57	1897 ± 59*
Na (mmol/L)	152 ± 4.7	124 ± 5.2*
K (mmol/L)	349.8 ± 10.0	285.2 ± 9.4*
Ca (mmol/L)	2.56 ± 0.22	2.21 ± 0.21
Cl (mmol/L)	228 ± 6.8	171 ± 7.4*
Urea (mmol/L)	1339 ± 43.6	1056 ± 34.0*
Creatinine (μmol/L)	5566 ± 312	4504 ± 232*
Vp (ng/ml)	0.93 ± 0.15	0.79 ± 0.11
pH	5.5 ± 0.1	5.8 ± 0.1
Serum	*Concentration*	
Osm (mOsm/kg H_2O)	307.3 ± 1.4	305.6 ± 1.8
Na (mmol/L)	142 ± 0.64	142 ± 0.53
K (mmol/L)	3.68 ± 0.10	3.72 ± 0.14
Ca (mmol/L)	2.06 ± 0.02	2.04 ± 0.03
Cl (mmol/L)	110.0 ± 0.69	109.8 ± 0.65
Urea (mmol/L)	9.27 ± 0.42	8.75 ± 0.34
Creatinine (μmol/L)	20.6 ± 0.7	21.1 ± 1.3
Glucose (mmol/L)	7.2 ± 0.4	8.7 ± 0.3*
Vp (ng/ml)	0.53 ± 0.03	0.63 ± 0.04*

FIG. 3. Analyses of the renal functions of $SCTR^{+/+}$ and $SCTR^{-/-}$ mice. (A) Representative images of renal tissues from $SCTR^{+/+}$ and $SCTR^{-/-}$ mice. $SCTR^{-/-}$ mice display urinary space enlargement (blue arrow), mesangial expansion, nodular glomerulosclerosis (yellow arrows), and medullary tubular dilation. There is also occasional clustering of mononuclear cells in the vicinity of tubular cells, indicating the presence of inflammatory responses in $SCTR^{-/-}$ mouse kidneys. PAS, periodic acid-Schiff staining; H&E, hematoxylin-and-eosin staining. (B) Urine and serum chemistries of $SCTR^{+/+}$ and $SCTR^{-/-}$ mice under ad libitum water conditions. Data are means ± standard errors ($n = 22$). *, $P < 0.05$ compared with age-matched wild-type mice. (C) Water intake and urinary output of wild-type (+/+), heterozygous (+/−), and knockout (−/−) mice. Wild-type ($n = 22$), heterozygous ($n = 24$), and knockout ($n = 22$) male mice were housed individually in metabolic cages for measurement of water consumption and urine excretion in a 24-h period. *, $P < 0.05$; **, $P < 0.01$.

stop codon, it would not be able to couple to intracellular signaling mechanisms. Taken together, these results show that targeted deletion of exon 10 in the m*SCTR* gene should give rise to a true null mutation in knockout animals.

Function of secretin and its receptor in the urinary system. $SCTR^{+/+}$, $SCTR^{+/-}$, and $SCTR^{-/-}$ mice were born at the expected 1:2:1 Mendelian ratio from the heterozygous parents, suggesting that no embryonic lethality was associated with the null mutant. $SCTR^{-/-}$ mice showed similar body weights at 12 weeks compared to those of their wild-type littermates ($SCTR^{+/+}$, 26.5 ± 1.5 g; $SCTR^{-/-}$, 25.5 ± 1.0 g), indicating no growth abnormality. Their general appearance and litter sizes were also similar to those of the wild-type mice.

To study putative renal functions of the receptor, kidneys from $SCTR^{+/+}$ and $SCTR^{-/-}$ mice were examined. The kidney/body weight ratio of $SCTR^{-/-}$ mice was significantly higher than that of the wild-type littermates (1.65-fold; 0.620 ± 0.034 g and 1.021 ± 0.086 g for $SCTR^{+/+}$ and $SCTR^{-/-}$, respectively; $n = 15$). Histological examination showed that $SCTR^{-/-}$ mice exhibited abnormalities in the renal cortex, as well as in the medulla, characterized by increased mesangial area, enlarged urinary space, and frequent tubular dilation and

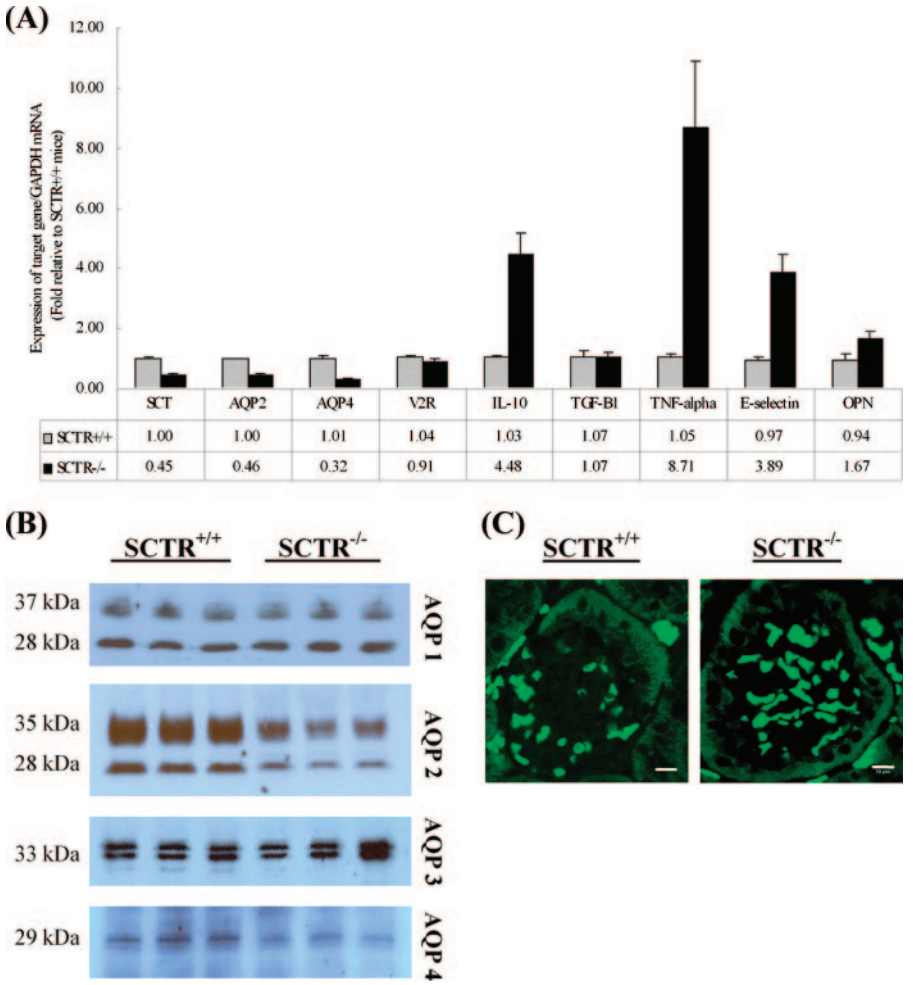

FIG. 4. (A) Relative mRNA expression levels of various genes in $SCTR^{+/+}$ and $SCTR^{-/-}$ mice given water ad libitum. The expression levels of various transcripts were measured by quantitative real-time reverse transcription-PCR, and the values were calculated by the $2^{-\Delta\Delta Ct}$ method relative to the corresponding levels in $SCTR^{+/+}$ mice. Data are the mean ± SEM of seven independent experiments performed in triplicate. SCT, secretin; AQP, aquaporin; V2R, Vp type 2 receptor; IL-10, interleukin-10; TGF-β1, transforming growth factor β1; TNF-α, tumor necrosis factor alpha; E-selectin, endothelial leukocyte adhesion molecule 1. *, $P < 0.05$; **, $P < 0.01$ (as determined by unpaired Student t test). (B) Representative images of the immunoblots of AQP1 to AQP4 in crude renal protein extracts of $SCTR^{+/+}$ and $SCTR^{-/-}$ mice with free access to water ($n = 9$). $SCTR^{-/-}$ mice expressed less AQP2 and AQP4 compared with $SCTR^{+/+}$ mice, while AQP1 and AQP3 levels were unchanged. (C) Immunofluorescent staining of F4/80 antigens in the kidneys of $SCTR^{+/+}$ and $SCTR^{-/-}$ mice. F4/80-positive macrophages were present at a higher concentration in the glomeruli of $SCTR^{-/-}$ mice, suggesting infiltration of macrophages. Bars, 10 μm.

hypertrophy in the collecting tubules of the medullary region (Fig. 3A), suggesting that they might have altered glomerular filtration and/or renal reabsorption processes. For this reason, we also measured water intake, urine output, and concentrations of Vp and various electrolytes in the urine and serum samples of euhydrating mice. As illustrated in Fig. 3B, the urine osmolality of $SCTR^{-/-}$ mice was significantly lower (decreased 17.3%) than that of $SCTR^{+/+}$ mice, indicating that the $SCTR^{-/-}$ animals produced more-diluted urine. Additionally, reductions in urinary Na^+ and K^+ excretion, as well as urea and creatinine levels, in the urine samples were also observed in the $SCTR^{-/-}$ mice. Nevertheless, serum concentrations of electrolyte, urea, and creatinine and creatinine clearance were not significantly different in $SCTR^{+/+}$ and $SCTR^{-/-}$ mice. In euhydrating animals, serum Vp levels were slightly higher in $SCTR^{-/-}$ mice, and this is consistent with the higher Vp transcript levels in the hypothalamuses of $SCTR^{-/-}$ mice (1.54-fold ± 0.19-fold; $P < 0.05$; $n = 20$). These data therefore suggest that the observed phenotypes developed by $SCTR^{-/-}$ mice were unlikely due to defects in Vp biosynthesis and/or secretion.

Figure 3C summarizes the amounts of water intake and urinary output of mice measured over a 24-h period. $SCTR^{-/-}$ mice exhibited polydipsia (45.5%, $P < 0.0001$) and polyuria (35.3%, $P < 0.0001$); they drank 8.0 ± 0.3 ml of water and produced 2.3 ± 0.1 ml of urine, compared to $SCTR^{+/+}$ mice, which drank 5.5 ± 0.3 ml of water and produced 1.7 ± 0.1 ml of urine. Conversely, heterozygous mice do not have the polyuric and polydipsic phenotypes, indicating that the abnormality stems completely from the lack of response to secretin. Taken together, our findings show that $SCTR^{-/-}$ mice have a disturbance in the process of water reabsorption and/or a higher probability of developing diabetes insipidus.

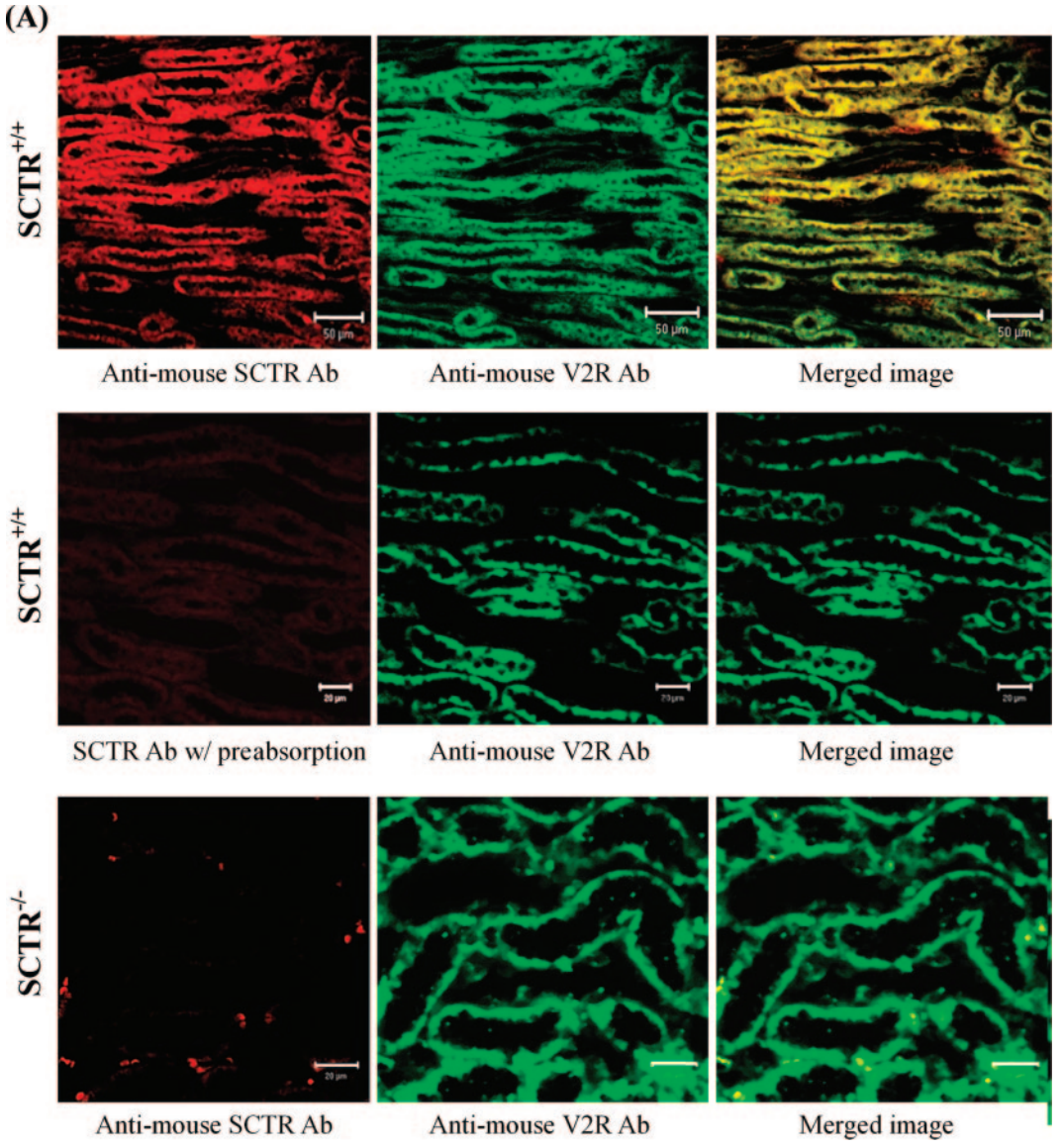

FIG. 5. Localization of SCTR in the kidney. SCTR immunoreactivities were primarily detected in the renal medulla, where it localized predominantly on the basolateral membranes of cells in the collecting ducts (blue arrow) and the ascending thick segments of the loop of Henle. (A) Upper part, confocal laser scanning images showing the localization of SCTR and V2R in the kidney tubular cells of $SCTR^{+/+}$ mice. Bars, 50 μm. Middle and bottom parts, control staining with 0.1 M antigen-preabsorbed SCTR antibody (Ab) in $SCTR^{+/+}$ mouse renal sections (i) and $SCTR^{-/-}$ mouse renal sections (ii). Bars, 20 μm. (B) Upper parts, photomicrographs showing the localization of SCTR and AQP2 in renal tissues. Middle and bottom parts, control staining with 0.1 M antigen-preabsorbed SCTR antibody in $SCTR^{+/+}$ mouse renal sections (i) and $SCTR^{-/-}$ mouse renal sections (ii). Bars, 20 μm.

Renal gene expression. The polyuric phenotype developed in $SCTR^{-/-}$ mice suggests possible biochemical changes in the kidney tubules. Figure 4A compares the expression levels of various genes, including those for secretin, aquaporins, Vp receptor, and various inflammatory markers in $SCTR^{+/+}$ and $SCTR^{-/-}$ mouse kidneys. Quantification by real-time reverse transcription-PCR revealed significant reductions in the transcript levels of secretin, AQP2, and AQP4, but not V2R, in the $SCTR^{-/-}$ kidney. This indicated that the impaired urine-concentrating ability of $SCTR^{-/-}$ mice is due not to reduced levels of V2R, and hence an altered response to Vp, but to reduced AQP2 and AQP4 expression levels. In accordance with these results, Western immunoblotting also revealed reduced expression of these aquaporins in the transgenic animals (Fig. 4B). As AQP2 and AQP4 were present on the apical and basolateral membranes, respectively, of the collecting tubules (33), reductions in both transcript and protein levels of these water channels were in agreement with the observed phenotypes developed by $SCTR^{-/-}$ animals.

Since we observed a higher blood glucose level (Fig. 3B) and pathological features that are characteristics of nephrogenic diabetes insipidus (NDI) in the kidneys of $SCTR^{-/-}$ mice, we investigated the expression of proinflammatory cytokines, as well as E-selectin and osteopontin (OPN), which are indicators

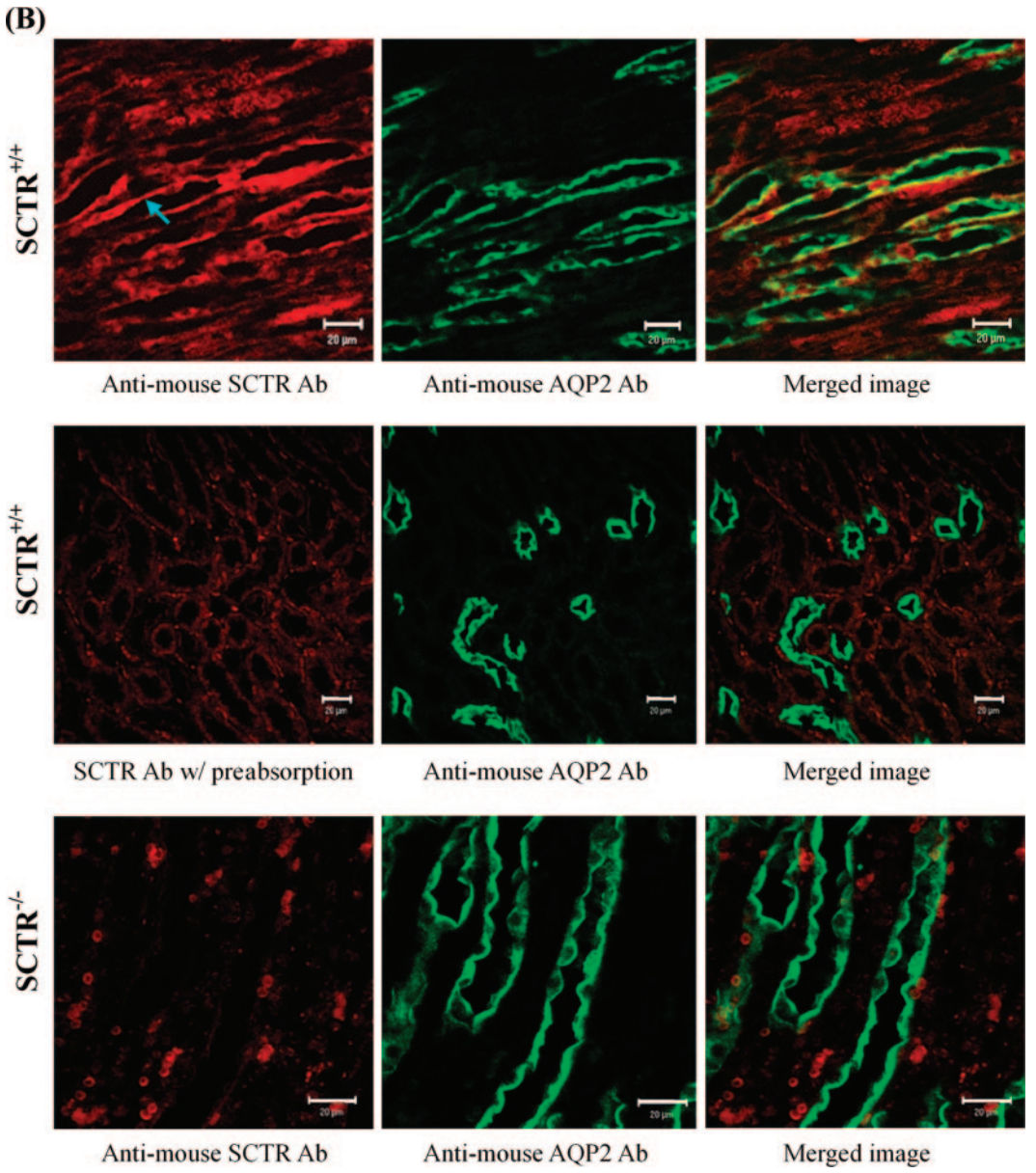

FIG. 5—*Continued*.

of inflammation and cell recruitment in diabetic nephropathy. Kidneys from $SCTR^{-/-}$ mice exhibited significant increases in transcript levels of interleukin-10, tumor necrosis factor alpha, E-selectin, and OPN, but not transforming growth factor β1, strongly suggesting a kidney damage condition in these mice (Fig. 4A). Moreover, $SCTR^{-/-}$ mice also showed an increased number of F4/80-positive cells, especially in the glomerulus (Fig. 4C). The infiltration of macrophages is likely a consequence of the increased expression of E-selectin, a mediator of macrophage infiltration, and OPN, a chemotactic factor of macrophages.

Effects of secretin on AQP2 trafficking in renal tubules. To understand further the direct actions of secretin on kidney tubules, we used renal sections from $SCTR^{+/+}$ mice, with $SCTR^{-/-}$ mice as negative controls, to examine the localization of SCTR, AQP2, and Vp receptor V2R (Fig. 5). Consistent with a previous report (7), immunohistochemical staining revealed the presence of SCTR in the renal medulla, where it was coexpressed with V2R in the cuboidal epithelium of the collecting ducts and in the simple columnar epithelium of the ducts of Bellini. In these regions, SCTR is predominantly found on the basolateral membrane while AQP2 is localized on the apical membrane. Additionally, we also observed the presence of SCTR in the proximal tubules and the ascending thick segment of the loop of Henle, suggesting a possible role for secretin in regulating Na^+ reabsorption.

As secretin could promote transepithelial solvent flux in cholangiocytes by activating AQP1 trafficking to the apical membrane (27, 28, 40), it is possible that this peptide could mimic the effect of Vp on AQP2 translocation in the renal

collecting tubules. Such a hypothesis could also explain the altered urine-concentrating ability of $SCTR^{-/-}$ mice. To address this, we examined the in vitro effects of secretin on the distribution of AQP2 in the inner medullary tubular cells of $SCTR^{+/+}$ and $SCTR^{-/-}$ mice. Figure 6A shows the relative abundances of AQP2 in the PM- and IV-enriched fractions isolated from these tubules after 30 min of secretin treatment. Secretin induced a dose-dependent increase in both the glycosylated and nonglycosylated AQP2 proteins in the PM of medullary tubules. Quantification of the blots revealed a 2.11-fold ± 0.15-fold increase in the PM/IV ratio of AQP2 after incubation with 10^{-8} M secretin. This effect, however, was not observed in the medullary tubules isolated from $SCTR^{-/-}$ mice, clearly indicating the specificity of the actions of secretin via its receptor.

The in vitro redistribution of AQP2 in renal tubules prompted us to examine the in vivo trafficking of AQP2 under chronic hyperosmotic conditions, again with $SCTR^{+/+}$ and $SCTR^{-/-}$ mice. Despite reductions in the overall abundance of AQP2, the PM/IV ratios in the kidneys of $SCTR^{+/+}$ and $SCTR^{-/-}$ mice were similar under ad libitum water conditions (0.82 ± 0.05 and 0.89 ± 0.06, respectively), with most of the AQP2 protein present in the IVs. Nevertheless, under water-deprived conditions, changes in the trafficking and expression of AQP2 were observed in $SCTR^{-/-}$ mice. As shown in Fig. 6B, water deprivation (60 h; $n = 8$) could trigger a 2.27-fold ± 0.27-fold increase in the shift of AQP2 from IVs to the PM and a 5.90-fold ± 1.06-fold increase in the AQP2 transcript level in $SCTR^{+/+}$ mice. These data are consistent with previous studies showing an increase in the overall abundance of AQP2 transcripts in the inner medulla of the kidney (30). In $SCTR^{-/-}$ mice, however, the effect of water deprivation on AQP2 trafficking and expression was significantly weaker (1.35-fold ± 0.16-fold and ~3.93-fold, respectively). These data clearly demonstrate that the induced expression and redistribution of AQP2 during water deprivation were at least partially dependent on SCTR, which represents an additional mechanism of the Vp-V2R axis.

Serum secretin levels during water deprivation. To substantiate the role of secretin in regulating renal water transport in response to water deprivation, we anticipated changes in serum secretin levels under hyperosmotic conditions. To examine this, we collected blood samples from $SCTR^{+/+}$ and $SCTR^{-/-}$ mice that had been deprived of drinking water for 2 days. In both $SCTR^{+/+}$ and $SCTR^{-/-}$ mice, circulating immunoreactive secretin levels were increased after water restriction (1.60-fold ± 0.03-fold and 1.58-fold ± 0.02-fold, respectively; $P < 0.05$) (Fig. 7). These elevations, however, were not significantly different in $SCTR^{+/+}$ and $SCTR^{-/-}$ mice, indicating that the differences in AQP2 trafficking and expression between $SCTR^{+/+}$ and $SCTR^{-/-}$ mice under water-deprived conditions are likely direct consequences of inadequate renal responses to secretin in the transgenic animals. Therefore, this finding, which shows an increase in serum secretin under hyperosmotic condition, affirms the osmoregulatory role of secretin hypothesized in this study.

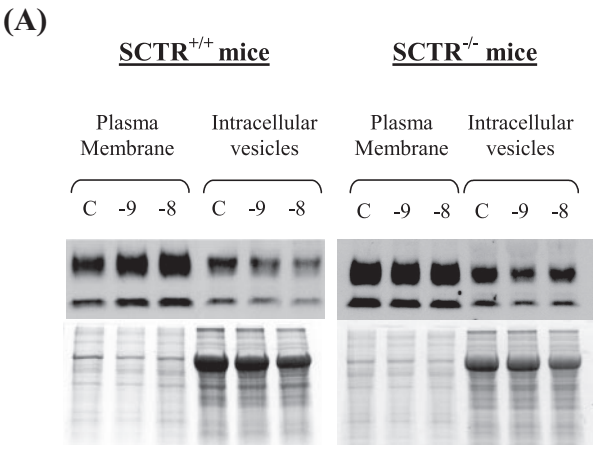

The effect of secretin on the redistribution of AQP2 in the inner medullary tubules isolated from $SCTR^{+/+}$ and $SCTR^{-/-}$ mice

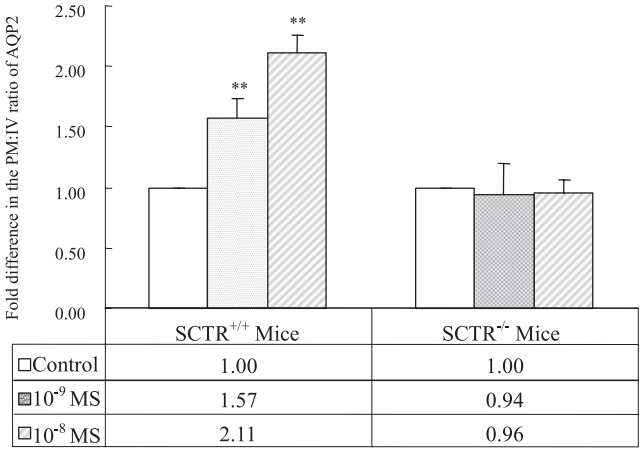

	SCTR+/+ Mice	SCTR-/- Mice
□Control	1.00	1.00
▨10-9 MS	1.57	0.94
□10-8 MS	2.11	0.96

DISCUSSION

Body water homeostasis is widely known to be regulated by AQP2, which plays a major role in renal water reabsorption and determines the concentration of urine. This is achieved by controlled insertion of AQP2 into the apical membrane of the collecting duct principal cells, where it acts as a hydrophilic pore to allow water to move transepithelially from the lumen to the interstitium and then subsequently to be reabsorbed via AQP3 and AQP4, which are located on the basolateral membrane. The regulation of AQP2 is based in part on the redistribution of AQP2-bearing vesicles to the apical membrane and in part on the changes in its overall abundance. These processes are predominantly regulated by the antidiuretic hormone Vp (34, 36) and the cAMP-responsive element in the 5′-flanking region of the gene for AQP2 (29). There is, however, evidence from both in vitro and in vivo studies indicating the presence of Vp-independent mechanisms regulating the translocation and expression of this water channel. The first piece of evidence came from the observation that 10 pM Vp, which is the highest plasma Vp concentration in severe dehydration, could only increase osmotic water permeability to 44% of the maximum (19). Factors other than Vp, therefore, could dramatically boost osmotic water permeability to levels much higher than that obtainable by Vp alone. Another piece of evidence came from a study of Vp-deficient Brattleboro rats.

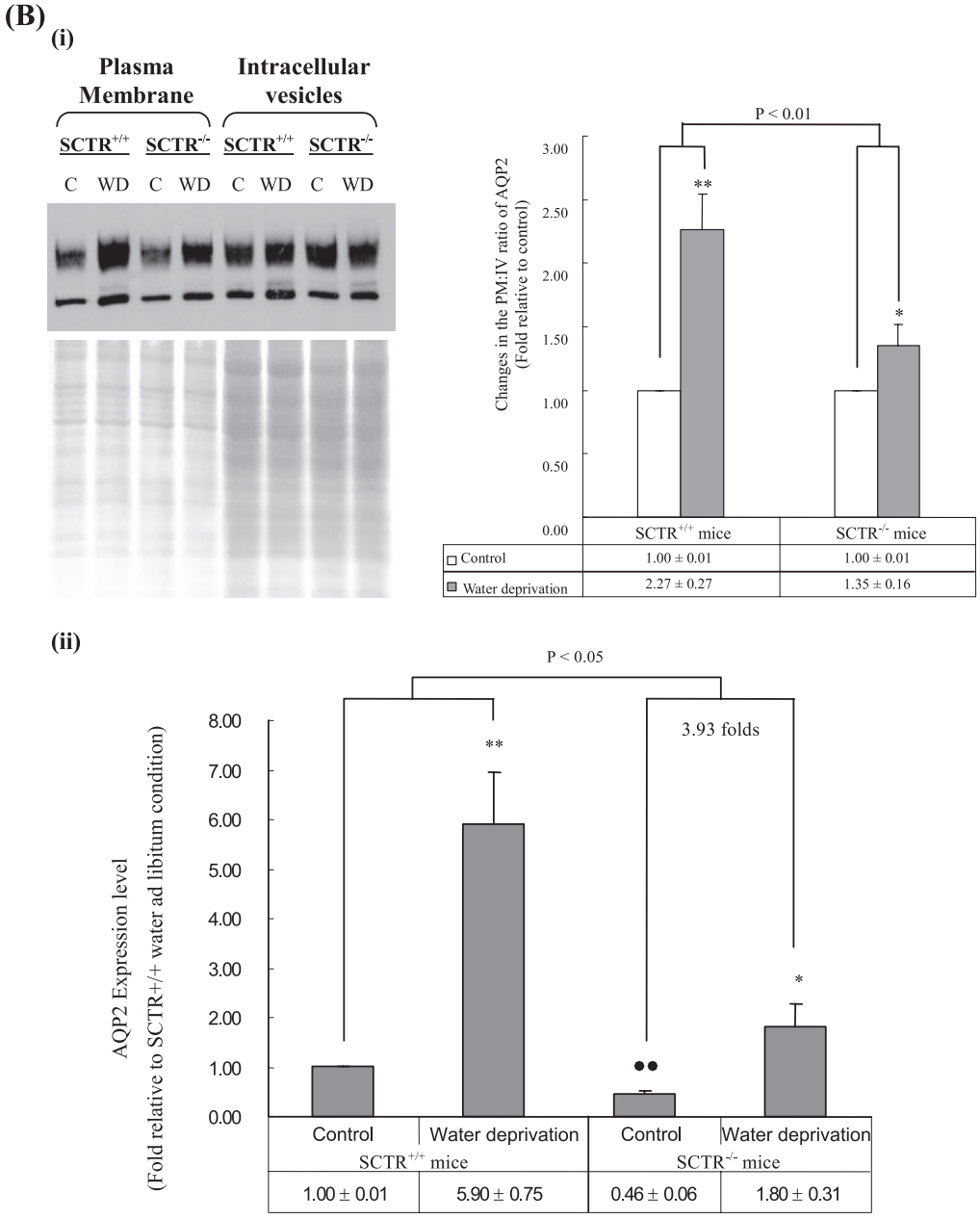

FIG. 6. (A) Effect of secretin on the subcellular localization of AQP2 in an inner medullar tubule suspension. The upper part shows immunoblots with the corresponding Coomassie blue-stained gels as loading controls (C). The bottom part shows densitometry analysis of the immunoblots. Values were calculated from the mean pixel intensity measured from the 35-kDa and 28-kDa bands (glycosylated and nonglycosylated AQP2, respectively). These were expressed as the fold changes in ratio between the intensities of the bands from PM and IVs. Secretin (S) treatment was shown to induce concentration-dependent trafficking of AQP2 from the IVs to the PM in tubules isolated only from wild-type animals. Statistical analyses of groups of samples run on the same gel were conducted. Results are from seven independent experiments. **, $P < 0.01$. (B) Renal responses of $SCTR^{+/+}$ and $SCTR^{-/-}$ mice under chronic hyperosmotic conditions. (i) Effect of water deprivation (WD) on the PM/IV ratio of AQP2 in the kidneys of $SCTR^{+/+}$ and $SCTR^{-/-}$ mice. The left part shows a representative immunoblot and a Coomassie blue-stained gel as a loading control. The right part shows the densitometry analysis of the immunoblots. Under ad libitum water conditions, the PM/IV ratios of AQP2 in the kidneys of $SCTR^{+/+}$ and $SCTR^{-/-}$ mice were similar (0.82 ± 0.05 and 0.89 ± 0.06, respectively), with most of the AQP2 proteins present in IVs. Under WD conditions, a significant shifting of AQP2 from IVs to the PM was observed in both $SCTR^{+/+}$ and $SCTR^{-/-}$ mice (PM/IV ratios, 1.86 ± 0.07 and 1.20 ± 0.08, respectively). Nevertheless, a significant reduction in the IV-to-PM translocation of AQP2 was observed in the kidneys of $SCTR^{-/-}$ mice ($P < 0.01$). Statistical analysis was conducted on groups of samples run on the same gel. Results were from eight independent experiments. *, $P < 0.05$; **, $P < 0.01$ (versus the control group). (ii) Effect of WD on renal AQP2 expression. Values are from five independent experiments and are expressed relative to the transcript levels of AQP2 in $SCTR^{+/+}$ mice under ad libitum water conditions. In $SCTR^{-/-}$ mice, WD could trigger an ~3.93-fold increase in the AQP2 transcript level, which is significantly less than that in $SCTR^{+/+}$ mice ($P < 0.05$). *, $P < 0.05$; **, $P < 0.01$ (versus the ad libitum water group); ●●, $P < 0.01$ (versus the ad libitum water $SCTR^{+/+}$ group).

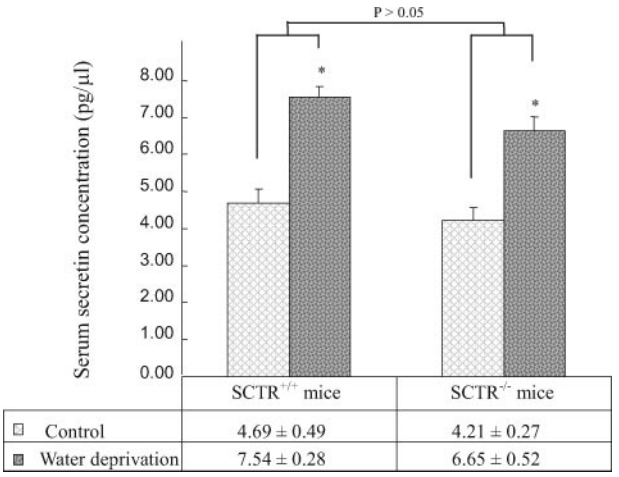

	$SCTR^{+/+}$ mice	$SCTR^{-/-}$ mice
Control	4.69 ± 0.49	4.21 ± 0.27
Water deprivation	7.54 ± 0.28	6.65 ± 0.52

FIG. 7. Effect of water deprivation on serum secretin levels. In both $SCTR^{+/+}$ and $SCTR^{-/-}$ mice, circulating immunoreactive secretin levels were increased 1.60-fold ± 0.03-fold and 1.58-fold ± 0.02-fold, respectively, after water restriction. Data are means ± SEMs for groups of seven or eight mice. *, $P < 0.05$ versus the ad libitum water group.

Li and colleagues showed that hyperosmolality in vivo in these animals could increase AQP2 expression and trafficking, as well as urinary osmolality (21), clearly indicating the presence of Vp-independent mechanisms in stimulating AQP2 expression and translocation. Hence, identifying factors that regulate the translocation and expression of AQP2 has important implications, as it provides insight into the fundamental physiology and pathophysiology of water homeostasis, as well as therapeutic potentials for disorders with the defect in water homeostasis, including NDI, heart failure, renal failure, and hypertension.

In this study, $SCTR^{-/-}$ mice were generated by deleting exon 10 of the gene, which encodes the third endoloop of the receptor, which is essential for G protein coupling and signal transduction. The renal morphologies observed in our studies, however, were not reported in the other transgenic secretin receptor mice that had exon 1 replaced with the *lacZ* reporter and a *PGKneobpA* selection marker (35). The discrepancies in our data are possibly due to differences in genetic background and/or the targeting strategies used in generating the transgenic animals. In our study, we used mice of the N5 generation while Nishijima et al. used mice that had a C57BL-6Jx129S7 mixed genetic background and gave no information regarding which generation of mice was used for experimentation. It is well documented that the genetic background of transgenic mice could influence the phenotypes developed and hence could sometimes lead to faulty interpretations of data (10, 14, 15, 23, 46). In addition, with the help of a secretin receptor antiserum recently raised in our laboratory (9), we were able to show genuine secretin receptor knockout in our mice, while in their study, they deleted exon 1, which should encode the signal peptide. Without any supporting data from immunohistochemical staining, it is therefore still possible that some functional secretin receptors are present in these animals. Further experiments are needed to investigate and clarify the phenotypic differences observed in these two types of secretin receptor knockout mice.

The observation of phenotypes such as polydipsia and polyuria in $SCTR^{-/-}$ mice raises the possibility that secretin might play a role in water homeostasis. In fact, the role of secretin and its receptor in regulating renal functions has been suggested but not fully substantiated in the past. One of the reasons is that the expression and localization of secretin receptors in the kidney were controversial. Previously, our laboratory showed that *SCTR* mRNA is expressed in the human kidney by Northern blot analysis (8) whereas Ulrich et al. (41) reported finding no expression of this receptor in the rat kidney by RNase protection assay. Charlton et al., on the other hand, found a high density of [^{125}I]secretin binding sites in the renal medulla (7). Moreover, inconsistent findings on the renal function of secretin have been reported. Early studies suggested a diuretic role for this peptide to increase renal excretion of water, bicarbonate, sodium, potassium, and calcium in normal humans and dogs (2, 3, 42, 43), whereas another study demonstrated an antidiuretic action of secretin when administered intravenously to anesthetized hydrated rats (7). In the latter study, secretin was shown to act on the receptor on the renal medulla to decrease urine output through the activation of adenylate cyclase, and this effect is as potent as that of Vp in Brattleboro rats. Consistent with these observations, the present study showed altered AQP2 expression and trafficking in $SCTR^{-/-}$ mice under water deprivation compared to that in $SCTR^{+/+}$ mice. These data not only corroborate the urine-concentrating ability and antidiuretic roles of secretin but also provide evidence, for the first time, that secretin could be one of the Vp-independent mechanisms controlling water homeostasis. Compatible with this idea, plasma secretin levels were found to increase three- to sixfold under stress (37), which is consistent with our finding that water restriction induces 5.66-fold ± 0.59-fold and 1.60-fold ± 0.03-fold plasma secretin level increases in rats (data not shown) and mice, respectively. Secretin, a classical hormone that controls the cellular transportation of electrolytes, is therefore a potential factor controlling AQP2 trafficking in the kidney and could serve as a potential candidate in treating X-linked NDI with defective V2R signaling. Consonant with this, $SCTR^{-/-}$ mice display pathological symptoms that are characteristics of NDI, such as polydipsia and excessive urination, glomerular hypertrophy, dilation of tubules in the renal medulla, down-regulation of AQP2 and AQP4 expression, up-regulation of E-selectin and OPN, and significant elevation of plasma Vp levels (11, 16–18, 20, 26, 32, 39, 45). Together with reported effects of secretin on insulin secretion (12, 13), alteration of the synthesis and/or secretion of this hormone might contribute to renal and metabolic perturbations observed in diabetes. Therefore, further investigation of secretin as a potential target for prevention and/or therapeutic intervention of this disease is warranted.

ACKNOWLEDGMENTS

We thank James Lau for ES cell injection and Leo L. T. Lee and Elisa Lau for excellent technical assistance.

This work was supported by Hong Kong government RGC grants HKU7501/05 M and HKU7384/04 M to Billy K. C. Chow.

REFERENCES

1. **Baiocchi, L., G. LeSage, S. Glaser, and G. Alpini.** 1999. Regulation of cholangiocyte bile secretion. J. Hepatol. **31:**179–191.
2. **Barbezat, G. O., J. I. Isenberg, and M. I. Grossman.** 1972. Diuretic action of secretin in dog. Proc. Soc. Exp. Biol. Med. **139:**211–215.
3. **Baron, D. N., F. Newman, and A. Warrick.** 1958. The effects of secretin on urinary volume and electrolytes in normal subjects and patients with chronic pancreatic disease. Experientia **14:**30–32.
4. **Bayliss, W. M., and E. H. Starling.** 1902. The mechanism of pancreatic secretion. J. Physiol. (London) **28:**325–353.
5. **Bradbury, N. A., and R. J. Bridges.** 1994. Role of membrane trafficking in plasma membrane solute transport. Am. J. Physiol. **267:**C1–C24.
6. **Chan, K. Y., R. T. Pang, and B. K. Chow.** 2001. Functional segregation of the highly conserved basic motifs within the third endoloop of the human secretin receptor. Endocrinology **142:**3926–3934.
7. **Charlton, C. G., R. Quirion, G. E. Handelmann, R. L. Miller, R. T. Jensen, M. S. Finkel, and T. L. O'Donohue.** 1986. Secretin receptors in the rat kidney: adenylate cyclase activation and renal effects. Peptides **7:**865–871.
8. **Chow, B. K.** 1995. Molecular cloning and functional characterization of a human secretin receptor. Biochem. Biophys. Res. Commun. **212:**204–211.
9. **Chow, B. K., K. H. Cheung, E. M. Tsang, M. C. Leung, S. M. Lee, and P. Y. Wong.** 2004. Secretin controls anion secretion in the rat epididymis in an autocrine/paracrine fashion. Biol. Reprod. **70:**1594–1599.
10. **Crusio, W. E.** 2004. Flanking gene and genetic background problems in genetically manipulated mice. Biol. Psychiatry **56:**381–385.
11. **Davis, F. B., and P. J. Davis.** 1981. Water metabolism in diabetes mellitus. Am. J. Med. **70:**210–214.
12. **Dupré, J., D. J. Chisholm, T. J. McDonald, and A. Rabinovitch.** 1975. Effects of secretin on insulin secretion and glucose tolerance. Can. J. Physiol. Pharmacol. **53:**1115–1121.
13. **Enk, B.** 1976. Secretin-induced insulin response. II. Dose-response relation. Acta Endocrinol. (Copenhagen) **82:**312–317.
14. **Gerlai, R.** 1996. Gene-targeting studies of mammalian behavior: is it the mutation or the background genotype? Trends Neurosci. **19:**177–181.
15. **Gerlai, R.** 2001. Gene targeting: technical confounds and potential solutions in behavioral brain research. Behav. Brain Res. **125:**13–21.
16. **Hirata, K., K. Shikata, M. Matsuda, K. Akiyama, H. Sugimoto, M. Kushiro, and H. Makino.** 1998. Increased expression of selectins in kidneys of patients with diabetic nephropathy. Diabetologia **41:**185–192.
17. **Hsieh, T. J., R. Chen, S. L. Zhang, F. Liu, M. L. Brezniceanu, C. I. Whiteside, I. G. Fantus, J. R. Ingelfinger, P. Hamet, and J. S. Chan.** 2006. Upregulation of osteopontin gene expression in diabetic rat proximal tubular cells revealed by microarray profiling. Kidney Int. **69:**1005–1015.
18. **Iwasaki, Y., K. Kondo, T. Murase, H. Hasegawa, and Y. Oiso.** 1996. Osmoregulation of plasma vasopressin in diabetes mellitus with sustained hyperglycemia. J. Neuroendocrinol. **8:**755–760.
19. **Jeon, U. S., K. W. Joo, K. Y. Na, Y. S. Kim, J. S. Lee, J. Kim, G. H. Kim, S. Nielsen, M. A. Knepper, and J. S. Han.** 2003. Oxytocin induces apical and basolateral redistribution of aquaporin-2 in rat kidney. Nephron Exp. Nephrol. **93:**e36–e45.
20. **Leung, J. C., L. Y. Chan, A. W. Tsang, S. C. Tang, and K. N. Lai.** 2005. Differential expression of aquaporins in the kidneys of streptozotocin-induced diabetic mice. Nephrology (Carlton) **10:**63–72.
21. **Li, C., W. Wang, S. N. Summer, M. A. Cadnapaphornchai, S. Falk, F. Umenishi, and R. W. Schrier.** 2006. Hyperosmolality in vivo upregulates aquaporin 2 water channel and Na-K-2Cl co-transporter in Brattleboro rats. J. Am. Soc. Nephrol. **17:**1657–1664.
22. **Li, X. M., and L. J. Shapiro.** 1993. Three-step PCR mutagenesis for 'linker scanning'. Nucleic Acids Res. **21:**3745–3748.
23. **Linder, C. C.** 2006. Genetic variables that influence phenotype. ILAR J. **47:**132–140.
24. **Livak, K. J., and T. D. Schmittgen.** 2001. Analysis of relative gene expression data using real-time quantitative PCR and the $2^{-\Delta\Delta Ct}$ method. Methods **25:**402–408.
25. **Lorenz, D., A. Krylov, D. Hahm, V. Hagen, W. Rosenthal, P. Pohl, and K. Maric.** 2003. Cyclic AMP is sufficient for triggering the exocytic recruitment of aquaporin-2 in renal epithelial cells. EMBO Rep. **4:**88–93.
26. **Makaryus, A. N., and S. I. McFarlane.** 2006. Diabetes insipidus: diagnosis and treatment of a complex disease. Clevel. Clin. J. Med. **73:**65–71.
27. **Marinelli, R. A., L. Pham, P. Agre, and N. F. LaRusso.** 1997. Secretin promotes osmotic water transport in rat cholangiocytes by increasing aquaporin-1 water channels in plasma membrane. Evidence for a secretin-induced vesicular translocation of aquaporin-1. J. Biol. Chem. **272:**12984–12988.
28. **Marinelli, R. A., P. S. Tietz, L. D. Pham, L. Rueckert, P. Agre, and N. F. LaRusso.** 1999. Secretin induces the apical insertion of aquaporin-1 water channels in rat cholangiocytes. Am. J. Physiol. **276:**G280–G286.
29. **Matsumura, Y., S. Uchida, T. Rai, S. Sasaki, and F. Marumo.** 1997. Transcriptional regulation of aquaporin-2 water channel gene by cAMP. J. Am. Soc. Nephrol. **8:**861–867.
30. **Michimata, M., S. Nogae, M. Ohta, S. Kaizuma, Y. Imai, S. Ito, and M. Matsubara.** 2000. Topographic distribution of aquaporin 2 mRNA in the kidney of dehydrated rats. Exp. Nephrol. **8:**28–36.
31. **Migeon, J. C., and N. M. Nathanson.** 1994. Differential regulation of cAMP-mediated gene transcription by m1 and m4 muscarinic acetylcholine receptors. Preferential coupling of m4 receptors to $G_i\alpha$-2. J. Biol. Chem. **269:**9767–9773.
32. **Narumi, S., M. L. Onozato, A. Tojo, S. Sakamoto, and T. Tamatani.** 2001. Tissue-specific induction of E-selectin in glomeruli is augmented following diabetes mellitus. Nephron **89:**161–171.
33. **Nejsum, L. N.** 2005. The renal plumbing system: aquaporin water channels. Cell. Mol. Life Sci. **62:**1692–1706.
34. **Nielsen, S., J. Frokiaer, D. Marples, T. H. Kwon, P. Agre, and M. A. Knepper.** 2002. Aquaporins in the kidney: from molecules to medicine. Physiol. Rev. **82:**205–244.
35. **Nishijima, I., T. Yamagata, C. M. Spencer, E. J. Weeber, O. Alekseyenko, J. D. Sweatt, M. Y. Momoi, M. Ito, D. L. Armstrong, D. L. Nelson, R. Paylor, and A. Bradley.** 2006. Secretin receptor-deficient mice exhibit impaired synaptic plasticity and social behavior. Hum. Mol. Genet. **15:**3241–3250.
36. **Noda, Y., and S. Sasaki.** 2005. Trafficking mechanism of water channel aquaporin-2. Biol. Cell **97:**885–892.
37. **Oektedalen, O., P. K. Opstad, and O. B. Schaffalitzky de Muckadell.** 1982. Secretin—a new stress hormone? Regul. Pept. **4:**213–219.
38. **Parvin, M. N., S. Kurabuchi, K. Murdiastuti, C. Yao, C. Kosugi-Tanaka, T. Akamatsu, N. Kanamori, and K. Hosoi.** 2005. Subcellular redistribution of AQP5 by vasoactive intestinal polypeptide in the Brunner's gland of the rat duodenum. Am. J. Physiol. Gastrointest. Liver Physiol. **288:**G1283–G1291.
39. **Tallroth, G., E. Ryding, R. Ekman, and C. D. Agardh.** 1992. The response of regulatory peptides to moderate hypoglycaemia of short duration in type 1 (insulin-dependent) diabetes mellitus and in normal man. Diabetes Res. **20:**73–85.
40. **Tietz, P. S., M. A. McNiven, P. L. Splinter, B. Q. Huang, and N. F. Larusso.** 2006. Cytoskeletal and motor proteins facilitate trafficking of AQP1-containing vesicles in cholangiocytes. Biol. Cell **98:**43–52.
41. **Ulrich, C. D., P. Wood, E. M. Hadac, E. Kopras, D. C. Whitcomb, and L. J. Miller.** 1998. Cellular distribution of secretin receptor expression in rat pancreas. Am. J. Physiol. **275:**G1437–G1444.
42. **Viteri, A. L., J. W. Poppell, J. M. Lasater, and W. P. Dyck.** 1975. Renal response to secretin. J. Appl. Physiol. **38:**661–664.
43. **Waldum, H. L., J. A. Sundsfjord, U. Aanstad, and P. G. Burhol.** 1980. The effect of secretin on renal haemodynamics in man. Scand. J. Clin. Lab. Investig. **40:**475–478.
44. **Wilke, C., S. Sheriff, M. Soleimani, and H. Amlal.** 2005. Vasopressin-independent regulation of collecting duct aquaporin-2 in food deprivation. Kidney Int. **67:**201–216.
45. **Yang, B., D. Zhao, L. Qian, and A. S. Verkman.** 2006. Mouse model of inducible nephrogenic diabetes insipidus produced by floxed aquaporin-2 gene deletion. Am. J. Physiol. Renal Physiol. **291:**465–472.
46. **Yoshiki, A., and K. Moriwaki.** 2006. Mouse phenome research: implications of genetic background. ILAR J. **47:**94–102.